JOC The Journal of Organic Chemistry

Article

pubs.acs.org/joc

The Biginelli Reaction Is a Urea-Catalyzed Organocatalytic Multicomponent Reaction

Maneeporn Puripat,[†,‡] Romain Ramozzi,[‡] Miho Hatanaka,[‡] Waraporn Parasuk,[§] Vudhichai Parasuk,[†,∥] and Keiji Morokuma*[,‡]

[†]Nanoscience and Technology Program, Graduate School, Chulalongkorn University, Bangkok 10330, Thailand

[‡]Fukui Institute for Fundamental Chemistry (FIFC), Kyoto University, Kyoto 606-8103, Japan

[§]Department of Chemistry, Faculty of Science, Kasetsart University, Bangkok 10900, Thailand

[∥]Department of Chemistry, Faculty of Science, Chulalongkorn University, Bangkok 10330, Thailand

Supporting Information

ABSTRACT: The recently developed artificial force induced reaction (AFIR) method was applied to search systematically all possible multicomponent pathways for the Biginelli reaction mechanism. The most favorable pathway starts with the condensation of the urea and benzaldehyde, followed by the addition of ethyl acetoacetate. Remarkably, a second urea molecule catalyzes nearly every step of the reaction. Thus, the Biginelli reaction is a urea-catalyzed multicomponent reaction. The reaction mechanism was found to be identical in both protic and aprotic solvents.

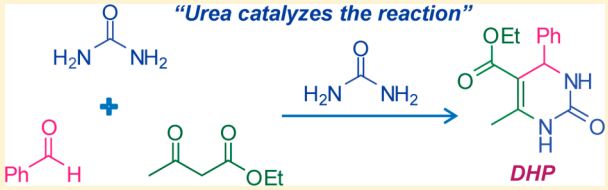

1. INTRODUCTION

Multicomponent reactions (MCRs) are reactions of three or more reactants in one pot leading to a product that ideally contains all atoms of the reactants.[1−10] These reactions have had great impact in organic synthesis due to atom and energy economy compared to linear synthesis.[11] Among these reactions, there are several types of MCRs such as MCRs involving isocyanide (Passerini[12−15] and Ugi coupling[16−18]) and MCRs involving acetoacetate (Biginelli[19,20] and Hantzsch reactions[21,22]).

The Biginelli reaction is one of the most essential MCRs[23−25] and known for the biological activities of its products,[25−27] such as anticancer,[28] antimalarial,[29] anti-HIV agents,[30] and others.[31−39] Discovered in 1893,[19,20] this reaction results in the condensation of three components: a urea, an aldehyde, and a β-keto ester to form the 4-aryl-3,4-dihydropyrimidin-2(1*H*)-one (**DHP**) as shown in Scheme 1.

To enhance the efficiency of the process, different variations of the experimental conditions[23] were proposed: the use of catalysts such as Brönsted[40−44] or Lewis acids,[10,45−48] ionic liquids,[49−54] or an excess of one reactant.[45,49,55−58] Soon after its discovery, various mechanisms involving protonated intermediates were proposed, as shown in Figure 1. The first mechanism, the so-called iminium route,[55] considers the condensation of the aldehyde and urea to form a C−N bond to give the iminium followed by a nucleophilic addition of the β-keto ester. The second mechanism, an enamine route,[9] starts from a urea and a β-keto ester to form a C−N bond to give the enamine, which reacts with the aldehyde. The third mechanism is a Knoevenagel type reaction[8] between the aldehyde and the β-keto ester to form a C−C bond before a reaction with the urea.

Scheme 1. Biginelli Reaction

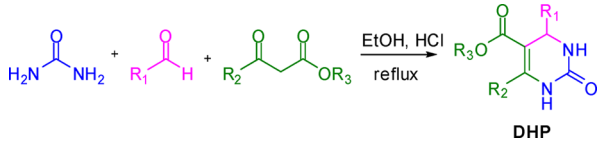

The reaction mechanism was discussed in various experimental and theoretical studies.[3,10,45,49,50,57−61] De Souza et al.[62] performed infusion electrospray ionization mass spectrometry (ESI-MS) to identify intermediates involved in the reaction. Different intermediates from all three routes were found. They complemented their study with a theoretical investigation for the C−C and C−N bonds formation steps and concluded that the iminium route was favored over the two others. The C−C bond formation, which corresponds to the nucleophilic addition of the β-keto ester on the iminium, was found to be the rate-determining step (RDS) of the process. More recently, Clark et al.[63] showed that the solvent ability to promote the tautomeric equilibrium for the β-keto ester impacts the process efficiency and that the proticity and polarity of the solvent are not critical, as the yields were found to be similar in ethanol and toluene for instance.

Various experimental findings mentioned above convinced us to clarify the preferred reaction pathway or pathways for a deep understanding of this important reaction. Are the three routes

Received: February 20, 2015
Published: June 11, 2015

DOI: 10.1021/acs.joc.5b00407
J. Org. Chem. 2015, 80, 6959−6967

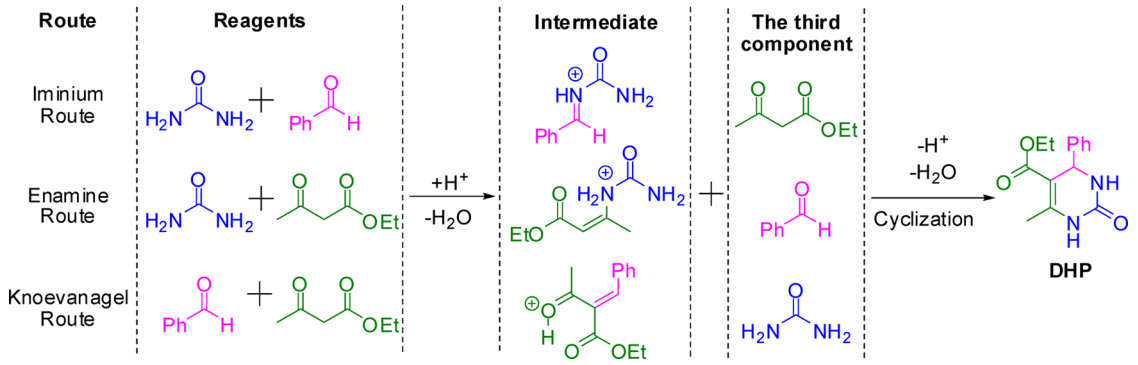

Figure 1. Three major possible mechanisms of the Biginelli reaction.

presented above the only possible pathways leading to the dihydropyrimidine? Is the mechanism strictly identical in protic and aprotic solvents? Does one of the reactants play the role of a catalyst? Unbiased and systematic studies of all possible reaction pathways involving various reactant molecules in different order (sometimes the same molecules two or more times) need to be performed to resolve these essential questions. The artificial force induced (AFIR) method developed recently by our group is ideally suited for this purpose.[64,65] In this method, an artificial force is placed randomly between reactants to find automatically all approximate transition states (TSs) and intermediates (local minima, LMs) of low-energy reaction pathways. From these approximate stationary points, true TSs and LMs are fully optimized without artificial force. This approach was used to investigate the 3-MCR, Passerini coupling,[66] which consists of the reaction between an aldehyde, an isocyanide, and a carboxylic acid to give an α-acyloxy amide. The AFIR approach demonstrated, contrary to the commonly accepted mechanism, that an additional carboxylic acid molecule is directly involved in the reaction and catalyzes the reaction.[14,15]

Herein, the mechanism of the Lewis acid catalyzed Biginelli reaction will be studied systematically using the AFIR method. The counterion will not be considered, as it is not directly involved in the reaction. Therefore, our search is not restricted to the proposed three mechanisms discussed above. For each pathway, we searched multicomponent pathways to examine possible involvement of additional components as catalysts. A preliminary search for three-body *concerted* pathways all seemed to converge to the two-body pathways, and thus, we did not pursue this approach further. In this research, we looked for all possible pathways including the C−C, C−N, or C−O bond at first from any one protonated reactant molecule and another unprotonated reactant molecule. We may note that reactions between two neutral reactants are not considered, as they have been found to have high barriers.[67] For instance, when the reaction starts from urea and aldehyde, the activation energy for the first condensation step was found to be 43.0 kcal mol^{-1}.

2. COMPUTATIONAL DETAILS

Urea, benzaldehyde, and ethyl acetoacetate are used to model the three reactants of the coupling. The detailed AFIR calculation scheme is as follows. As the first bond formation step (Step I), alternately choosing one protonated reactant and another neutral reactant, an artificial force is placed between all intermolecular atom pairs since we still have no idea on how the reaction really occurs. Additionally, concerted processes with simultaneous bond forming and breaking are also considered. At first, approximate reaction paths (AFIR paths) were searched extensively for all approach directions and orientation, and approximate local minimums (LMs) and transition states structures (TSs) were located.[64,65,68] The relative orientations and approach directions of the two reactants were generated randomly.[65] The artificial force (AF) energy parameter used was γ = 200 kJ mol^{-1}, which suggests that pathways with a barrier of more than 50 kcal mol^{-1} will not be searched. The initial AFIR search was made using the M06-2X/3-21G level of theory. The AFIR search was terminated when no new AFIR LM was found for N_{max} consecutive AFIR paths. Here, different conformations of LMs are of course considered to be new and different. In this study, N_{max} = 10 was used; although not exhaustive nor guaranteed because of the nature of the method, past experiences[64,68] suggest that essential pathways are not likely to be missed using this value of N_{max}. The obtained pathways are always inspected manually for obvious omission. Then, from these approximate structures, *true* LMs and TSs were reoptimized *without artificial force* at the M06-2X/6-31+G(d) level. It is important to emphasize that, in order to clarify the possible catalytic role of extra reactant molecules, many multicomponent pathways involving extra reactant and solvent molecules were searched with the AFIR method and will be presented in the Results and Discussion section.

We report in the Results and Discussion section the Gibbs free energy (at 1 atm and 298.15 K; no change in conclusions at 348.15 K, the boiling point of ethanol) and the electronic energy with zero-point correction (ZPE, in parentheses). There are different arguments concerning the entropy contributions in solution, some suggesting scaling and others suggesting truncation; the reality seems to lie between the two extremes.[69−81] Since we plan to compare mainly different potential energy profiles with the same number of reactant molecules, the difference between the Gibbs free energy and electronic energy with ZPE is rather small. In the text, we mainly use the Gibbs free energy.

For Step II, the dehydration from the first intermediates takes place in two steps. Whatever the pathway, no concerted pathway was found. For the proton transfer sub-Step IIA, we apply the AF (γ = 200 kJ mol^{-1}) repulsively (negative value of γ) between the atoms where a bond is expected to be broken and attractively between the atoms where a bond is expected to be formed. The same principle was used for the dehydration sub-Step IIB and for Steps III and IV discussed below.

In all calculations, the solvation Gibbs free energy was included by the polarized continuum model (PCM). For the initial AFIR search with M06-2X/3-21G, a PCM model using the dielectric constant of 24.9 for ethanol was employed. Then, all approximate TSs and LMs were reoptimized at M06-2X/6-31+G(d) using the same PCM model. In section 3.5 (Solvent Dependency), the pathways of Route **A**, **B**, and **C** in PCM toluene were optimized from the most favorable pathways obtained in ethanol. Moreover, the effect of solvent proticity was considered in the proton transfer steps by considering explicit solvent molecule(s) in ethanol.

After optimization of a TS, the intrinsic reaction coordinate (IRC)[82,83] was calculated to confirm the reaction pathway. IRC from a TS structure leads to a reactant or product complex, which is not necessarily the lowest conformation. Usually, the barrier from these

DOI: 10.1021/acs.joc.5b00407
J. Org. Chem. 2015, 80, 6959−6967

IRC derived conformations is not very high, and we just connected the lowest and less stable conformers without calculation of the TS between them. All these AFIR searches, optimizations, and IRC calculations were performed with the Global Reaction Route Mapping (GRRM)[84−86] program using energies, first, and, second, energy derivatives computed with the Gaussian09 program.[87]

3. RESULTS AND DISCUSSION

In the following sections, we will discuss three routes separately: Route **A** starts the reaction with the protonated urea and benzaldehyde, Route **B** with the protonated urea and ethyl acetoacetate, and Route **C** with the protonated ethyl acetoacetate and benzaldehyde. In each route, we followed the initial bond formation step between two reactants (Step I), dehydration step (Step II), bond formation step with the third component (Step III), and final transformation step into **DHP** (Step IV). It is important to emphasize that, for all steps, we considered multicomponent pathways carefully to examine possible involvement of the additional reactant or solvent molecule as catalysts.

3.1. Route A, Starting with Reaction of Protonated Urea and Benzaldehyde. *3.1.1. Step I: Initial Bond Formation.* At first, the initial protonation always takes place on urea because of its high proton affinity (see Figure S1 in the Supporting Information (SI)). All calculations starting with protonated benzaldehyde result in the same reaction pathways as those with protonated urea.

The first step of this route is the reaction between the protonated urea and benzaldehyde. Three pathways (**A1**−**A3**) were found as shown in Figure 2. Among them, the C−O bond

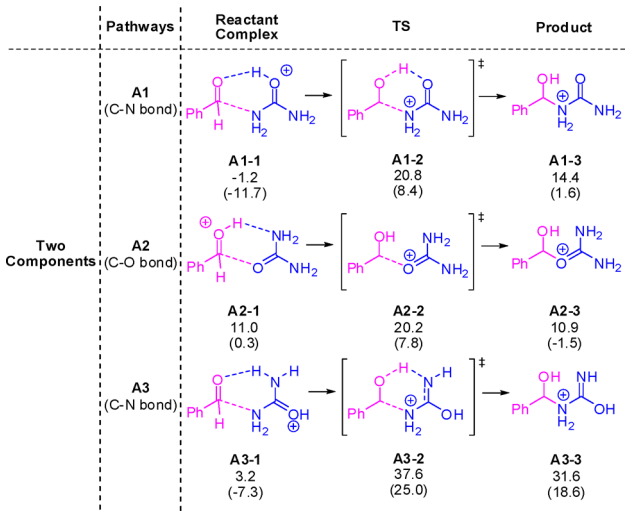

Figure 2. Intermediates and transition states between protonated urea and benzaldehyde (Step I in Route **A**). Gibbs free energies (1 atm, 298.15 K) (electronic energies with ZPE correction in parentheses), in kcal mol^{-1} relative to the isolated reactant molecules, were obtained at the M06-2X/6-31+G(d) level in PCM ethanol.

formation (**A2**) has the lowest TS (**A2-2**) with a 20.2 kcal mol^{-1} activation barrier. The IRC from this TS leads to the reactant complex (**A2-1**), higher in energy than the complex (**A1-1**) because of a smaller proton affinity of benzaldehyde than urea. The second lowest pathway is the C−N bond formation (**A1**) to give an iminium intermediate. This TS **A1-2** is only 0.6 kcal mol^{-1} higher than **A2-2**. IRC shows that, in this path, the proton transfer from the urea oxygen to the benzaldehyde oxygen takes place concertedly with the C−N bond formation between the urea amine group and the benzaldehyde carbonyl carbon. The pathway **A3** is much higher in energy and can be ignored.

To form the final product **DHP**, a C−N bond between these two partners has to be formed. The AFIR search found no concerted process to form the C−N bond from **A2-3**. In order to consider a possible catalytic process, a second urea was added to react with **A2-3** (see Scheme 2 and Figure S2 in the

Scheme 2. Proposed Catalytic Process with a Second Urea (in Red Circle)

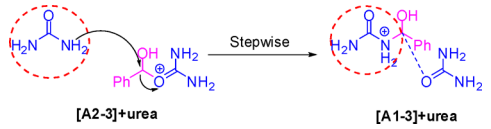

SI). The reaction proceeds in a stepwise process. The C−O bond originally formed has to dissociate before forming the new C−N bond between the second urea and benzaldehyde. The lowest TS for this pathway is 5.5 kcal mol^{-1} higher than the TS of the direct C−N bond formation (**A1-2**). Therefore, we conclude that the best path for Step I of pathway **A** is the direct C−N bond formation (**A1**) from the resting stage (**A1-1**) of the reactant complex.

In order to consider the possible involvement of additional components in this reaction step, we further examined their effects on the pathway **A1**. Figure 3 shows the most stable conformations for three- and four-component reactions; other less stable conformations are shown in the Supporting Information (Figures S3−S4). For the three-component reaction, an extra urea, benzaldehyde, and *β*-keto ester, respectively, were added to the LMs and TS of pathway **A1**, as shown as pathway **A1U**, **A1Z**, and **A1E**. With the benzaldehyde or ethyl acetoacetate as a third component (**A1Z** and **A1E**), the resulting TS structures are essentially similar to the ones without an extra reactant but stabilize the acidic proton on the benzaldehyde. This results in an increase of the nucleophilicity of the urea and electrophilicity of the benzaldehyde involved in the C−N bond formation. Surprisingly, an additional urea lowers the energy of the resulting TS (**A1U-2**), compared to **A1-2**. The Gibbs free energy of this TS is 15.5 kcal mol^{-1}, which is 5.3 kcal mol^{-1} lower than that of **A1-2** without the extra urea. The main difference resides in the position of the proton. While in **A1** the proton was bonded to the reacting urea, it is now bonded to the additional urea in the **A1U** pathway. The hydrogen bonding with the extra protonated urea stabilizes the system, and the urea nitrogen involved in the C−N bond formation becomes more nucleophilic, compared to pathway **A1**, and explains the stabilization of the TS. We can conclude that *an extra urea molecule catalyzes this step of the Biginelli reaction*. This is consistent with the observation that an excess of urea is often used experimentally.

To consider the effects of ethyl acetoacetate on the LM and TS in pathway **A1U**, the four-component reaction pathway (**A1UE**), which considers all three reactants and the extra urea, is then investigated. We found that the barriers of **A1U** and **A1UE** are similar and that the ethyl acetoacetate just stabilizes the proton on the nitrogen, which is not directly involved in the reaction. In addition, a third urea (**A1UU**) or a second benzaldehyde (**A1UZ**) in the four components step was also considered (see Figure S5 in the SI). Their role is similar to

DOI: 10.1021/acs.joc.5b00407
J. Org. Chem. 2015, 80, 6959−6967

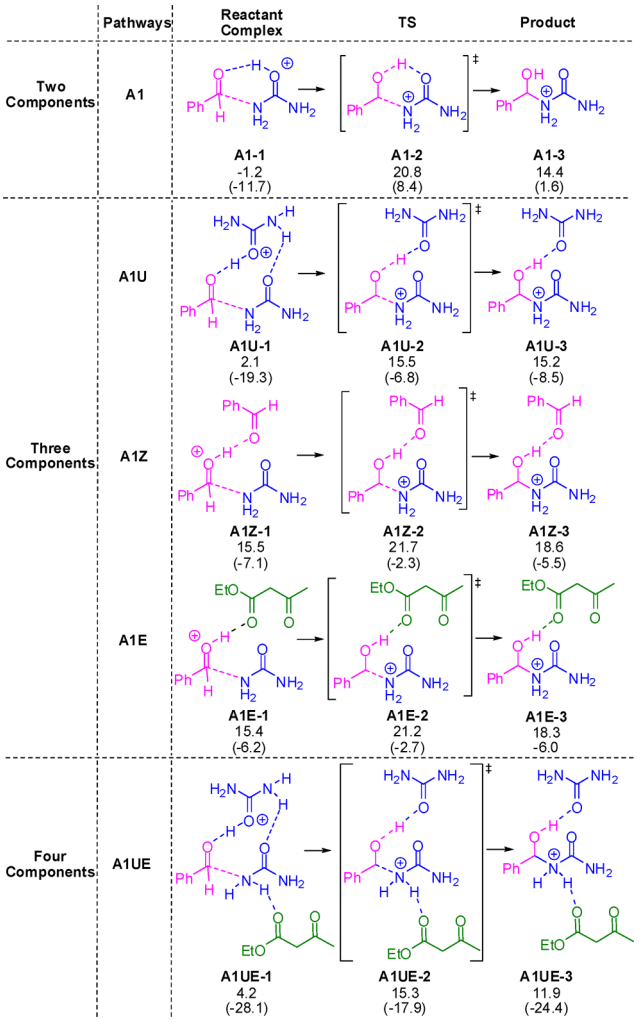

Figure 3. Two-, three-, and four-component Step I (C−N bond formation) for Route **A**. See Figure 2 for computational details.

that of the additional ethyl acetoacetate in **A1UE**. Thus, we can say that the fourth component is not directly involved in the reaction.

3.1.2. Step II: Dehydration. Now, we consider the dehydration step (Step II) from the intermediate **A1-3**, which results in formation of the iminium cation observed in ESI-MS.[62] The direct dehydration of **A1-3** without the "catalyst" did not take place in the AFIR search. Possible participation of protic molecules, water, one, and, two, ethanol molecules, has also been examined. However, water or ethanol has been found not to participate positively in the reaction, if compared to urea. The pathways are 6.5, 4.1, and 3.9 kcal mol^{-1} higher than the urea-catalyzed pathway, as shown in Figure S6 and Table S1 in the SI. As shown in Figure 4, we found that the extra urea catalyzes this pathway and the reaction takes place stepwise. Starting from the most stable conformer **A1UE-3′** of the intermediate of Step I, the proton transfer from the tertiary nitrogen of the reacted urea part to the extra urea carbonyl oxygen takes place with a very low barrier to give **A1UE-5**. This intermediate then isomerizes easily to give **A1UE-5′**, which goes over the TS **A1UE-6** to give the iminium ion **A1UE-7** coordinated with the water, ethyl acetoacetate, and urea products.

We conclude this section by saying that the extra urea molecule catalyzes Step II, as well as Step I discussed above.

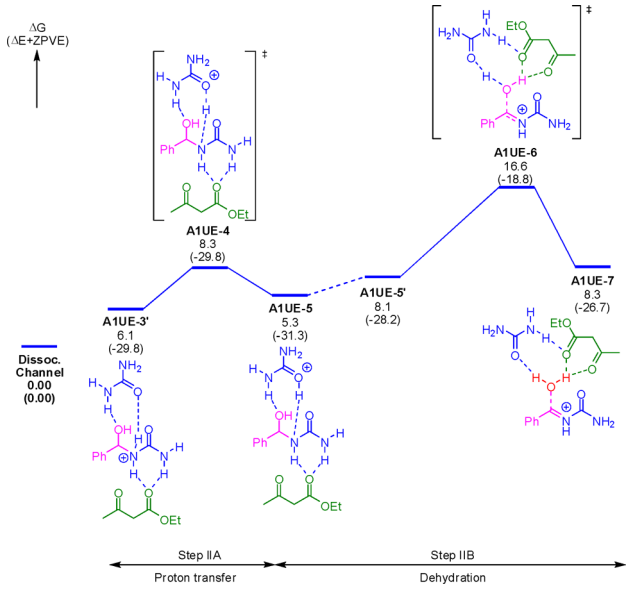

Figure 4. Most favorable pathways of Step II (Route **A**). See Figure 2 for computational details. The straight dashed line shows intermediates that are not connected by IRC.

3.1.3. Step III: Bond Formation with Ethyl Acetoacetate. After the dehydration step, the C−C bond formation between the intermediate **A1-4** (Figure S6) and ethyl acetoacetate was considered. In solution, the β-keto ester can tautomerize into the corresponding enol, as shown in Figure 5. Although the

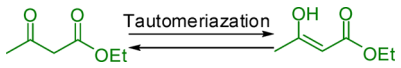

Figure 5. Diketo−enol tautomerization of an ethyl acetoacetate.

keto form is more stable (~4 kcal mol^{-1}), the enol form is needed for the C−C bond formation with **A1-4**. This is consistent with the experimental fact that the reaction efficiency is proportional to the diketo−enol tautomerization equilibrium constant (K_T).[63] The most stable TS (**A1UE-10**) for the C−C bond formation including an extra urea (see Figure 6) is only 1.9 kcal mol^{-1} lower than the TS without extra urea (Figure S7). However, the addition of the extra urea stabilizes the product of this step by 12.5 kcal mol^{-1}. In summary, while the extra urea is not directly involved in this step, it stabilizes the resulting product as it works as a strong proton acceptor from the ethyl acetoacetate part.

An alternative reaction pathway including the extra urea was examined. Indeed, according to the ESI-MS analyses,[62] a diurea derivative (**A1-6** in Figure 7 and Figure S8 in the SI) formed by a benzaldehyde and two urea molecules was observed. We found that the energies of **A1-6** and its formation TS are 10.4 and 20.8 kcal mol^{-1}, respectively. Thus, the formation of **A1-6** can take place, but the product **DHP** cannot be formed from it. The energy of the TS for the C−C bond formation with ethyl acetoacetate is 36.7 kcal mol^{-1}, too high if compared to **A1UE-10**. Thus, the diurea intermediate **A1-6** is a dead-end side product, which cannot be converted to the **DHP** product without going back to **A1-4**.

3.1.4. Step IV: Transformation into DHP. The transformation of **A1UE-11** into **DHP** consists of several steps as shown in Figure 6. First, the cyclization takes place, which is followed by a proton transfer from the extra urea to the enol

DOI: 10.1021/acs.joc.5b00407
J. Org. Chem. 2015, 80, 6959−6967

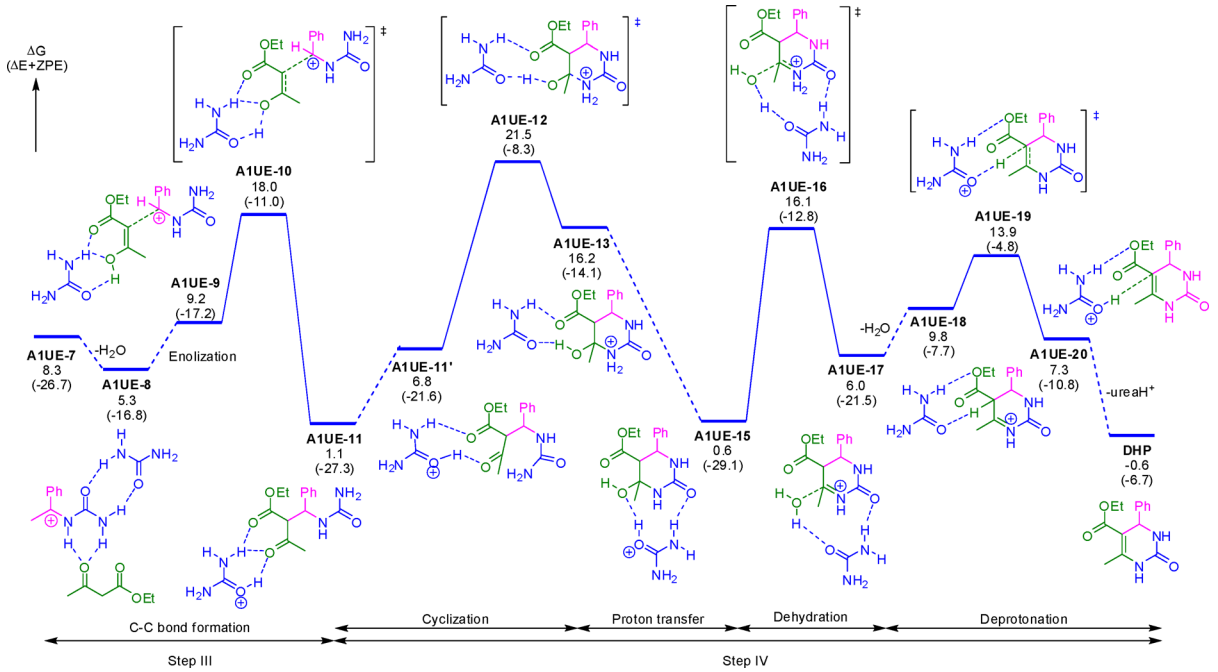

Figure 6. Most favorable pathways of Step III and IV (Route **A**) starting from **A1UE-7** to **DHP**. Figure 2 for computational details. The straight dashed line shows intermediates that are not connected by IRC.

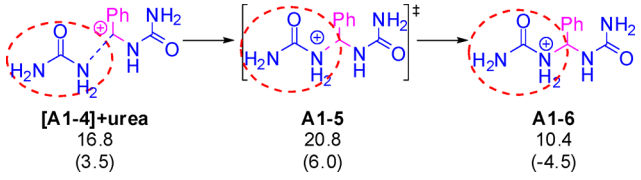

Figure 7. C−N bond formation leading to diurea derivative (**A1-6**). See Figure 2 for computational details.

part. Then the dehydration step and the deprotonation step by the extra urea result in the formation of **DHP**. The RDS of Route **A** is the cyclization substep in step IV, whose reaction barrier through the TS, **A1UE-12**, is 21.5 kcal mol^{-1}. This result is different from the results of the previous theoretical study.[62] In this study, it was concluded that the C−C bond formation (Step III) was the RDS, but the cyclization step, the real RDS, was not investigated in the calculation. The TS of the RDS, **A1UE-12**, is modestly stabilized by the extra urea as shown in Figure 6 (and Figure S9 in SI). The energy of the

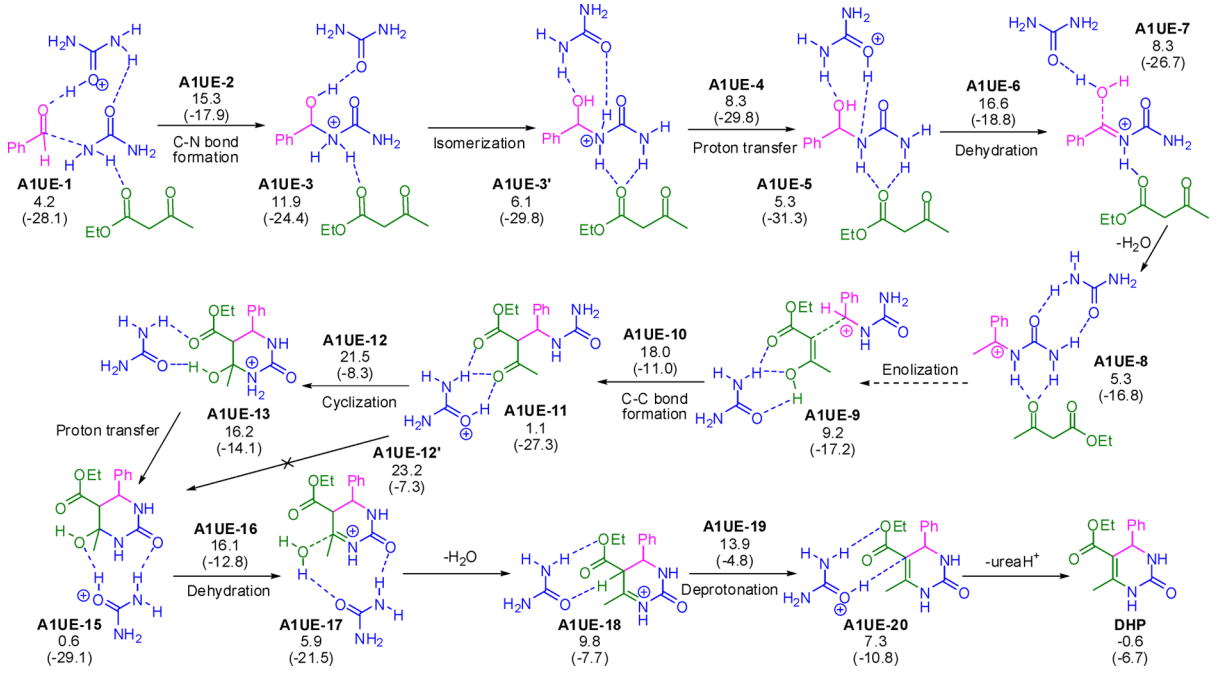

Figure 8. Best overall pathway for Route **A**. See Figure 2 for computational details.

DOI: 10.1021/acs.joc.5b00407
J. Org. Chem. 2015, 80, 6959−6967

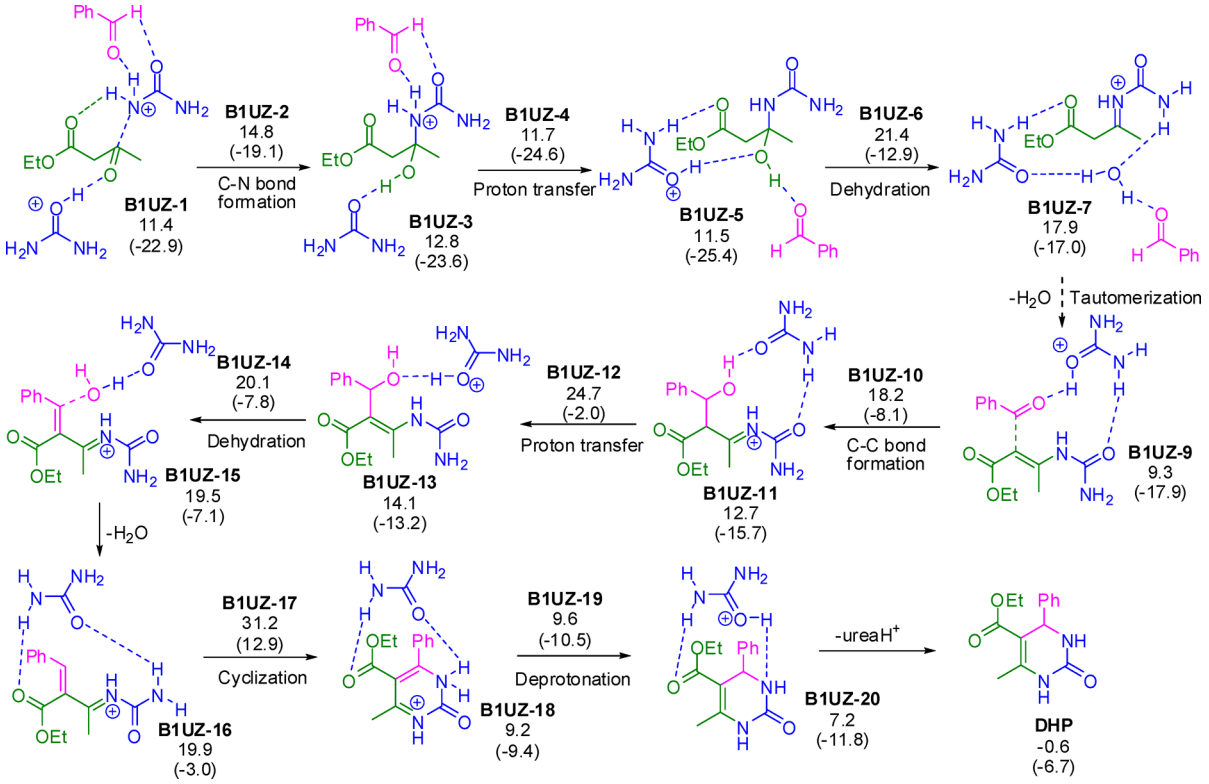

Figure 9. Best pathway for Route **B**. See Figure 2 for computational details.

cyclization TS without an extra urea, **A1E-12**, is 2.2 kcal mol^{-1} higher than that of **A1UE-12**. The extra urea also promotes the succeeding proton transfer and dehydration steps. The concerted pathway leading to **A1UE-15** from **A1UE-12′** was also considered during AFIR process but requires a 1.7 kcal mol^{-1} higher barrier in Figure 8 (and Figure S10 in SI) than the stepwise pathway. As already discussed in the Step II, the additional urea mediates proton transfer and dehydration steps better than protic solvent molecules such as water and ethanol. The TS for dehydration with the extra urea (**A1UE-16**) is 4.7 kcal mol^{-1} more stable than that with ethanol (**A1E-16+EtOH**). *We conclude this section by saying that the extra urea molecule catalyzes Step IV.*

3.1.5. Overall Pathway in Route A. Figure 8 shows the best overall pathway for Route **A**. The additional urea lowers the energies of nearly all the TSs along Route **A**. This explains why an excess of urea is sometimes chosen experimentally.[9,10,58,59,88−90] *Urea acts as an efficient oraganocatalyst in this* reaction. This is consistent with the experimental fact that the proticity and polarity of the solvent are not critical.[63] Moreover, the cyclization step is the RDS of this route. While ΔG_r is very small for the reaction, the Biginelli reaction product is not soluble under these conditions and is obtained as a solid. Therefore, we consider this reaction as irreversible and consider the higher TS structure (**A1UE-12**) as rate-determining. Before this step, the tautomerization of the *β*-keto ester into the enol, followed by the C−C bond formation step, has to occur. This pathway is thus consistent with experimental results that the efficiency of this reaction is affected by an enolization of the *β*-keto ester.[63]

The electronic effects of the aryl group of the aldehyde were also considered by adding an electron-withdrawing group (EWG, $-NO_2$) or an electron-donating group (EDG, −OMe) in the para position of the benzaldehyde for all three pathways. As detailed in Table S2, pathway **A** remains the best pathway and the RDS barriers are similar regardless of the substituents. Thus, the aryl ring substitution of the aldehyde has a small influence on the reaction. This result is consistent with the experiments.[63]

3.2. Route B, Starting with Reaction of Protonated Urea and Ethyl Acetoacetate. For Route **B**, urea and ethyl acetoacetate were considered for the initial condensation and each reactant was protonated alternatively. Additional components were considered at each step of the process to ensure that the best pathway is obtained. All AFIR pathways are summarized in the Supporting Information (Figures S11−S14 and Table S3). The best pathway in Route **B** is **B1** as shown in Figure 9. The lowest pathway for the initial C−N bond formation is stabilized by the additional urea and benzaldehyde, whose energy of the TS, **B1UZ-2**, is 14.8 kcal mol^{-1}. The resulting intermediate, **B1UZ-3**, is then dehydrated in a two-step process. The dehydration is promoted by the extra urea again. The energy of the TS is 21.4 kcal mol^{-1}, which is lower than the same step catalyzed by other molecules (see Figure S13 and Table S3). After tautomerization of this intermediate into the enamine **B1UZ-9**, the C−C bond formation occurs with a 18.2 kcal mol^{-1} barrier to reach **B1UZ-11**. During this step, the extra urea activates the aldehyde. The barrier with the extra urea is 8.7 kcal mol^{-1} lower than that without the extra urea. The consecutive dehydration is promoted by urea to form **B1UZ-16**. The cyclization step is the RDS for Route **B**, as in Route **A**. Various conformations and catalysts were considered to promote this cyclization (see Figure S15 in the SI). The lowest transition state structure shown in Figure 9 involves an extra urea to increase the nucleophilicity of the nitrogen involved in the C−N bond formation to provide **B1UZ-18**. A 31.2 kcal mol^{-1} overall barrier was found for this key step. After isomerization, the expected product is obtained.

DOI: 10.1021/acs.joc.5b00407
J. Org. Chem. 2015, 80, 6959−6967

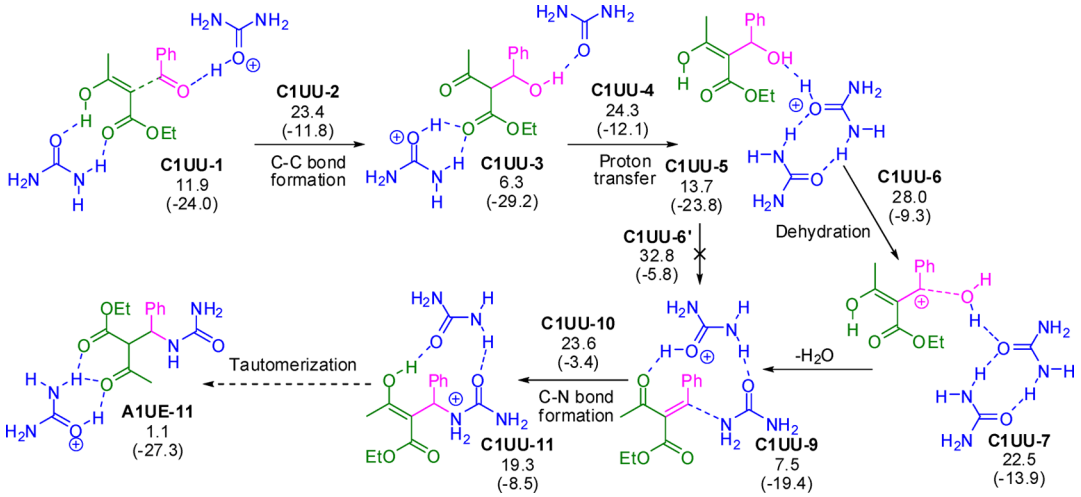

Figure 10. Best pathway for Route **C** (Step I–IV) leading to **A1UE-11**. See Figure 2 for computational details.

3.3. Route C, Starting with Reaction of Protonated Ethyl Acetoacetate and Benzaldehyde. For Route **C**, the benzaldehyde and ethyl acetoacetate (alternatively protonated) are considered as the first reactants for the condensation. All AFIR-searched pathways are summarized in Supporting Information (Figures S16–S20, Table S4 in SI). With a similar approach to the one used in routes **A** and **B**, only the best pathway is discussed here in Figure 10. The best four-component pathway leading to the C–C bond formation is through TS **C1UU-2**, with a 23.4 kcal mol^{-1} activation energy. Among all tested extra molecules, urea remains to be the best one to catalyze the dehydration steps. When ethanol molecules (the solvent) or two molecules of urea are used, the energy of the process is increased. The highest point along Route **C** is the C–O bond breaking TS **C1UU-6**, with an overall Gibbs free energy of 28.0 kcal mol^{-1}, which is rate-determining for Route **C**. In this case, a concerted pathway leading to **C1UU-9** from **C1UU-6′** was considered but requires a higher barrier (32.8 kcal mol^{-1}) (Figure S19). The next step consists of the condensation of the urea with the dehydrated intermediate **C1UU-7** to lead to **A1UE-11**, which is a common intermediate with Route **A**. Thus, the final steps, which consist of the cyclization and dehydration steps, were already discussed in section 3.1.4.

3.4. Comparison of All Routes. All the routes, **A** (iminium), **B** (enamine), and **C** (Knoevenagel), found by using the AFIR exploration method are similar to the ones proposed over the past decades, and no new route was found. However, it is noteworthy to mention that the participation of an extra urea is essential to lower the barriers for nearly all the steps. The best four-component pathways for three routes can be seen individually in Figures 8, 9, and 10, for Routes **A**, **B**, and, **C**, respectively. They are all combined and systematically compared in Figure S21 in the SI. The analysis of the two first steps shows that Routes **A** and **B** are in competition. While Route **B** has the lowest TS energy for this first step, one can notice that the dehydration process of the resulting intermediate (**B1UZ-3**) is much higher than that in Route **A**. Table 1 summarizes the highest point on the reaction pathway or the RDS of each route. Route **A** is 6.5 and 9.7 kcal mol^{-1} lower in energy than Routes **C** and **B**, respectively. It is interesting to note that the RDSs are different from those proposed in the previous studies in which not all the steps have been examined. The RDSs for Routes **A** and **B** correspond to the cyclization step at the end of the process, while it is the dehydration step for Route **C**. In this work, the lowest reactant is common for all the routes **A**, **B**, and **C**. Thus, we can discuss the rate based on the $\Delta G^{\ddagger}$ of the TSs.

Table 1. Energies (in kcal mol^{-1}) of the Transition States of the Rate-Determining Step for the Different Routes

Route: Rate-Determining Step	$\Delta G^{\ddagger}$
Route **A**: Cyclization/C–N bond formation (**A1UE-12**)	21.5
Route **B**: Cyclization/C–N bond formation (**B1UZ-17**)	31.2
Route **C**: dehydration step/C–O bond breaking (**C1UU-6**)	28.0

3.5. Solvent Dependency. As already mentioned, ethanol and toluene provide similar yields despite their different polarity and proticity properties.[63] As detailed in the previous section, ethanol is not directly involved in the mechanism, as urea is more efficient for all the proton transfers. To confirm that the reaction proceeds with a similar mechanism in toluene and ethanol, the three routes were reoptimized in toluene from the pathways optimized in ethanol (see Figures S22–S24 and Table S5). Intermediates and transition state structures were found to be qualitatively close to the ones obtained in ethanol. As the lowest reactant is common for all the Routes **A**, **B**, and **C**, we can discuss the rate based on the $\Delta G^{\ddagger}$ of the TSs. Table S5 summarizes the highest point on the reaction pathway or the RDS of each route. Route **A** is still the most favorable pathway, which is 9.6 and 1.8 kcal mol^{-1} lower in energy than Route **B** and **C**, respectively. Even though, the RDSs of Route **C** is different from those proposed in ethanol in which C–N bond formation (step III) become the RDS, while the RDSs for routes **A** and **B** corresponds to the cyclization step, the conclusion remains still the same. Thus, the reaction proceeds with a similar mechanism in ethanol and toluene, as the proticity of the solvent is not involved in the minimum energetic pathway (especially in the dehydration steps). A 22.0 kcal mol^{-1} activation barrier was calculated in toluene for Route **A**, which is close to the 21.5 kcal mol^{-1} one calculated in ethanol. This result is consistent with experimental results,[63] and we conclude that a similar mechanism is followed in ethanol and toluene.

DOI: 10.1021/acs.joc.5b00407
J. Org. Chem. 2015, 80, 6959–6967

4. CONCLUSIONS

In this study, we investigated for the first time the entire reaction mechanism of the Biginelli reaction starting from benzaldehyde, urea, and ethyl acetoacetate as reactants by using the recently developed artificial force induced reaction (AFIR) method,[64,65] combined with DFT calculations. Among all possibilities, three main routes were found to be suitable to lead to the expected product, the dihydropyrimidinone (**DHP**). The first route, the iminium Route **A**, starts with a reaction between the benzaldehyde and urea followed by the condensation of the ethyl acetoacetate. The rate-determining step of this reaction is, contrary to common belief,[62] the C−N bond formation during the cyclization step with a 21.5 kcal mol^{-1} overall barrier. The second route, the enamine Route **B**, results in the condensation of the urea with ethyl acetoacetate before the condensation of the benzaldehyde. While the RDS is still the cyclization step, the resulting barrier was found to be about 10 kcal mol^{-1} higher in energy than that in Route **A**. The last route, the so-called Knoevenagel Route **C**, starts with the condensation between the benzaldehyde and ethyl acetoacetate. However, the formation of the corresponding intermediate is the RDS and is about 6.5 kcal mol^{-1} higher in energy than the RDS of Route **A**.

The most important finding here is that nearly all steps of all the routes are catalyzed by an extra urea. The role of the extra urea is to stabilize the Lewis acid, as well as to reserve a proton; the urea accepts and releases protons as needed during the process. Therefore, the Biginelli reaction is a urea-catalyzed multicomponent reaction. Overall, the urea-catalyzed iminium pathway **A** is the most favorable pathway for the Biginelli reaction.

Solvent molecules are not involved in the reaction mechanism as much as urea is involved, even when a protic solvent is considered (e.g., ethanol). In ethanol, the RDS is still the C−N bond formation step with a very similar TS structure and energy, as this result explains why similar yields can be obtained experimentally both in protic and aprotic solvents.[63]

In the present study, we used the simplest reactants, namely, urea, benzaldehyde, and ethyl acetoacetate. However, we expect these three routes to remain the major ones with modestly substituted reactants. With very bulky substituents, the best pathway may change because of close contacts among reactants. Consequently, designing Biginelli reactions with different substituents and catalysts would be an interesting and challenging subject.

■ ASSOCIATED CONTENT

Supporting Information

Additional reaction pathways, and Cartesian coordinates and energies for all of the calculated structures related to this manuscript. The Supporting Information is available free of charge on the ACS Publications website at DOI: 10.1021/acs.joc.5b00407.

■ AUTHOR INFORMATION

Corresponding Author

*E-mail: morokuma.keiji.3a@kyoto-u.ac.jp.

Notes

The authors declare no competing financial interest.

■ ACKNOWLEDGMENTS

The authors are grateful to Prof. Satoshi Maeda of Hokkaido University for the developmental version of the GRRM code. P.M. gratefully acknowledges support by the Development and Promotion of Science and Technology Talents Project (DPST) (Royal Government of Thailand scholarship) of Thailand. R.R. thanks the Japan Society for the Promotion of Science (JSPS) for a fellowship. This work was partly supported by Grants-in-Aid for Scientific Research <KAKENHI> (Nos. 24245005, 26105733, and 15H02158) at Kyoto University. The Computer resources at the Institute for Information Management and Communication (IIMC) of Kyoto University and at the Research Center of Computer Science (RCCS) at the Institute for Molecular Science are also acknowledged.

■ REFERENCES

(1) Dömling, A. *Chem. Rev.* **2006**, *106*, 17−89.
(2) Dömling, A.; Ugi, I. *Angew. Chem., Int. Ed.* **2000**, *39*, 3168−3210.
(3) Alvim, H. G. O.; da Silva Júnior, E. N.; Neto, B. A. D. *RSC Adv.* **2014**, *4*, 54282−54299.
(4) Bienaymé, H.; Hulme, C.; Oddon, G.; Schmitt, P. *Chem.—Eur. J.* **2000**, *6*, 3321−3329.
(5) Ugi, I.; Werner, B.; Dömling, A. *Molecules* **2003**, *8*, 53−66.
(6) Dömling, A.; Wang, W.; Wang, K. *Chem. Rev.* **2012**, *112*, 3083−3135.
(7) Santos, V. G.; Godoi, M. N.; Regiani, T.; Gama, F. H. S.; Coelho, M. B.; de Souza, R. O. M. A.; Eberlin, M. N.; Garden, S. J. *Chem.—Eur. J.* **2014**, *20*, 12808−12816.
(8) Sweet, F.; Fissekis, J. D. *J. Am. Chem. Soc.* **1973**, *95*, 8741−8749.
(9) Folkers, K.; Johnson, T. B. *J. Am. Chem. Soc.* **1933**, *55*, 3784−3791.
(10) Cepanec, I.; Litvić, M.; Filipan-Litvić, M.; Grüngold, I. *Tetrahedron* **2007**, *63*, 11822−11827.
(11) Cioc, R. C.; Ruijter, E.; Orru, R. V. A. *Green Chem.* **2014**, *16*, 2958−2975.
(12) Passerini, M.; Simone, L. *Gazz. Chim. Ital.* **1921**, *51*, 126−129.
(13) Passerini, M.; Ragni, G. *Gazz. Chim. Ital.* **1931**, *61*, 964−969.
(14) Maeda, S.; Komagawa, S.; Uchiyama, M.; Morokuma, K. *Angew. Chem.* **2011**, *123*, 670−675.
(15) Ramozzi, R.; Morokuma, K. *J. Org. Chem.* **2015**, *80*, 5652−5657.
(16) Ugi, I.; Meyr, R.; Fetzer, U.; Steinbrückner, C. *Angew. Chem.* **1959**, *71*, 386−388.
(17) Ugi, I.; Steinbrückner, C. *Angew. Chem.* **1960**, *72*, 267−268.
(18) Chéron, N.; Ramozzi, R.; El Kaïm, L.; Grimaud, L.; Fleurat-Lessard, P. *J. Org. Chem.* **2012**, *77*, 1361−1366.
(19) Biginelli, P. *Gazz. Chim. Ital.* **1893**, *23*, 360−416.
(20) Biginelli, P. *Ber. Dtsch. Chem. Ges.* **1893**, *26*, 447.
(21) Hantzsch, A. *Ber. Dtsch. Chem. Ges.* **1881**, *14*, 1637−1638.
(22) Hantzsch, A. *Justus Liebigs Ann. Chem.* **1882**, *215*, 1−82.
(23) Sandhu, S.; Sandhu, J. S. *ARKIVOC* **2012**, 66−133.
(24) Biginelli, P. *Gazz. Chim. Ital.* **1889**, *19*, 212.
(25) Kappe, C. O. *Eur. J. Med. Chem.* **2000**, *35*, 1043−1052.
(26) Kappe, C. O. *Tetrahedron* **1993**, *49*, 6937−6963.
(27) Tron, G. C.; Minassi, A.; Appendino, G. *Eur. J. Org. Chem.* **2011**, *2011*, 5541−5550.
(28) Raju, B. C.; Rao, R. N.; Suman, P.; Yogeeswari, P.; Sriram, D.; Shaik, T. B.; Kalivendi, S. V. *Bioorg. Med. Chem. Lett.* **2011**, *21*, 2855−2859.
(29) Chiang, A. N.; Valderramos, J.-C.; Balachandran, R.; Chovatiya, R. J.; Mead, B. P.; Schneider, C.; Bell, S. L.; Klein, M. G.; Huryn, D. M.; Chen, X. S.; Day, B. W.; Fidock, D. A.; Wipf, P.; Brodsky, J. L. *Bioorg. Med. Chem.* **2009**, *17*, 1527−1533.
(30) Patil, A. D.; Kumar, N. V.; Kokke, W. C.; Bean, M. F.; Freyer, A. J.; Brosse, C.; De Mai, S.; Truneh, A.; Faulkner, D. J.; Carte, B.; Breen, A. L.; Hertzberg, R. P.; Johnson, R. K.; Westley, J. W.; Potts, B. C. M. *J. Org. Chem.* **1995**, *60*, 1182−1188.

DOI: 10.1021/acs.joc.5b00407
J. Org. Chem. 2015, 80, 6959−6967

(31) Lloyd, J.; Finlay, H. J.; Atwal, K.; Kover, A.; Prol, J.; Yan, L.; Bhandaru, R.; Vaccaro, W.; Huynh, T.; Huang, C. S.; Conder, M.; Jenkins-West, T.; Sun, H.; Li, D.; Levesque, P. *Bioorg. Med. Chem. Lett.* **2009**, *19*, 5469−5473.
(32) Agbaje, O. C.; Fadeyi, O. O.; Fadeyi, S. A.; Myles, L. E.; Okoro, C. O. *Bioorg. Med. Chem. Lett.* **2011**, *21*, 989−992.
(33) Lewis, R. W.; Mabry, J.; Polisar, J. G.; Eagen, K. P.; Ganem, B.; Hess, G. P. *Biochemistry* **2010**, *49*, 4841−4851.
(34) Rajanarendar, E.; Reddy, M. N.; Murthy, K. R.; Reddy, K. G.; Raju, S.; Srinivas, M.; Praveen, B.; Rao, M. S. *Bioorg. Med. Chem. Lett.* **2010**, *20*, 6052−6055.
(35) Mokale, S. N.; Shinde, S. S.; Elgire, R. D.; Sangshetti, J. N.; Shinde, D. B. *Bioorg. Med. Chem. Lett.* **2010**, *20*, 4424−4426.
(36) Trivedi, A. R.; Bhuva, V. R.; Dholariya, B. H.; Dodiya, D. K.; Kataria, V. B.; Shah, V. H. *Bioorg. Med. Chem. Lett.* **2010**, *20*, 6100−6102.
(37) Chitra, S.; Devanathan, D.; Pandiarajan, K. *Eur. J. Med. Chem.* **2010**, *45*, 367−371.
(38) Alam, O.; Khan, S. A.; Siddiqui, N.; Ahsan, W.; Verma, S. P.; Gilani, S. J. *Eur. J. Med. Chem.* **2010**, *45*, 5113−5119.
(39) Rajesh, S. M.; Kumar, R. S.; Libertsen, L. A.; Perumal, S.; Yogeeswari, P.; Sriram, D. *Bioorg. Med. Chem. Lett.* **2011**, *21*, 3012−3016.
(40) Gorobets, N. Y.; Sedash, Y. V.; Ostras, K. S.; Zaremba, O. V.; Shishkina, S. V.; Baumer, V. N.; Shishkin, O. V.; Kovalenko, S. M.; Desenko, S. M.; Van der Eycken, E. V. *Tetrahedron Lett.* **2010**, *51*, 2095−2098.
(41) Světlík, J.; Kettmann, V. *Tetrahedron Lett.* **2011**, *52*, 1062−1066.
(42) Cho, H.; Nishimura, Y.; Yasui, Y.; Kobayashi, S.; Yoshida, S.; Kwon, E.; Yamaguchi, M. *Tetrahedron* **2011**, *67*, 2661−2669.
(43) Hassani, Z.; Islami, M. R.; Kalantari, M. *Bioorg. Med. Chem. Lett.* **2006**, *16*, 4479−4482.
(44) Tu, S. J.; Zhu, X. T.; Fang, F.; Zhang, X. J.; Zhu, S. L.; Li, T. J.; Shi, D. Q.; Wang, X. S.; Ji, S. J. *Chin. J. Chem.* **2005**, *23*, 596−598.
(45) Ramos, L. M.; Ponce, A. Y.; Leon, D.; Santos, M. R.; Oliveira, H. C. B.; De Gomes, A. F.; Gozzo, F. C.; Oliveira, A. L.; De Neto, B. A. D. *J. Org. Chem.* **2012**, *77*, 10184−10193.
(46) Singh, O. M.; Devi, N. S. *J. Org. Chem.* **2009**, *74*, 3141−3144.
(47) Hu, E. H.; Sidler, D. R.; Dolling, U. *J. Org. Chem.* **1998**, *63*, 3454−3457.
(48) Maiti, G.; Kundu, P.; Guin, C. *Tetrahedron Lett.* **2003**, *44*, 2757−2758.
(49) Alvim, H. G. O.; Lima, T. B.; de Oliveira, H. C. B.; de Gozzo, F. C.; Macedo, J. L.; de Abdelnur, P. V.; Silva, W. A.; Neto, B. A. D. *ACS Catal.* **2013**, *3*, 1420−1430.
(50) Ramos, L. M.; Guido, B. C.; Nobrega, C. C.; Corrêa, J. R.; Silva, R. G.; Oliveira, Heibbe C. B. de; Gomes, A. F.; Gozzo, F. C.; Neto, B. A. D. *Chem.—Eur. J.* **2013**, *19*, 4156−4168.
(51) Kore, R.; Srivastava, R. *J. Mol. Catal. A: Chem.* **2011**, *345*, 117−126.
(52) Joseph, J. K.; Jain, S. L.; Singhal, S.; Sain, B. *Ind. Eng. Chem. Res.* **2011**, *50*, 11463−11466.
(53) Peng, X. C. Y. *Catal. Lett.* **2008**, *122*, 310−313.
(54) Li, M.; Guo, W. S.; Wen, L. R.; Li, Y. F.; Yang, H. Z. *J. Mol. Catal. A: Chem.* **2006**, *258*, 133−138.
(55) Kappe, C. O. *J. Org. Chem.* **1997**, *62*, 7201−7204.
(56) Xu, D. Z.; Li, H.; Wang, Y. *Tetrahedron* **2012**, *68*, 7867−7872.
(57) Alvim, H. G. O.; Lima, T. B.; de Oliveira, A. L.; de Oliveira, H. C. B.; Silva, F. M.; Gozzo, F. C.; Souza, R. Y.; da Silva, W. A.; Neto, B. A. D. *J. Org. Chem.* **2014**, *79*, 3383−3397.
(58) Shen, Z. L.; Xu, X. P.; Ji, S. J. *J. Org. Chem.* **2010**, *75*, 1162−1167.
(59) Litvić, M.; Večenaj, I.; Ladišić, Z. M.; Lovrić, M.; Vinković, V.; Filipan Litvić, M. *Tetrahedron* **2010**, *66*, 3463−3471.
(60) Kamal Raj, M.; Rao, H. S. P.; Manjunatha, S. G.; Sridharan, R.; Nambiar, S.; Keshwan, J.; Rappai, J.; Bhagat, S.; Shwetha, B. S.; Hegde, D.; Santhosh, U. *Tetrahedron Lett.* **2011**, *52*, 3605−3609.
(61) Atwal, K. S.; Rovnyak, G. C.; Reilly, B. C. O.; Schwartz, J. *J. Org. Chem.* **1989**, *54*, 5898−5907.
(62) De Souza, R. O. M. A.; da Penha, E. T.; Milagre, H. M. S.; Garden, S. J.; Esteves, P. M.; Eberlin, M. N.; Antunes, O. A. C. *Chem.—Eur. J.* **2009**, *15*, 9799−9804.
(63) Clark, J. H.; Macquarrie, D. J.; Sherwood, J. *Chem.—Eur. J.* **2013**, *19*, 5174−5182.
(64) Maeda, S.; Morokuma, K. *J. Chem. Theory Comput.* **2011**, *7*, 2335−2345.
(65) Maeda, S.; Morokuma, K. *J. Chem. Phys.* **2010**, *132*, 241102.
(66) Maeda, S.; Komagawa, S.; Uchiyama, M.; Morokuma, K. *Angew. Chem., Int. Ed.* **2011**, *50*, 644−649.
(67) Ma, J. G.; Zhang, J. M.; Jiang, H. H.; Ma, W. Y.; Zhou, J. H. *Chin. Chem. Lett.* **2008**, *19*, 375−378.
(68) Maeda, S.; Ohno, K.; Morokuma, K. *Phys. Chem. Chem. Phys.* **2013**, *15*, 3683−3701.
(69) Tanaka, R.; Yamashita, M.; Chung, L. W.; Morokuma, K.; Nozaki, K. *Organometallics* **2011**, *30*, 6742−6750.
(70) Huang, F.; Lu, G.; Zhao, L.; Li, H.; Wang, Z. X. *J. Am. Chem. Soc.* **2010**, *132*, 12388−12396.
(71) Lau, J. K.; Deubel, D. V. *J. Chem. Theory Comput.* **2006**, *2*, 103−106.
(72) Štrajbl, M.; Sham, Y. Y.; Villà, J.; Chu, Z. T.; Warshel, A. J. *J. Phys. Chem. B* **2000**, *104*, 4578−4584.
(73) Mammen, M.; Shakhnovich, E. I.; Deutch, J. M.; Whitesides, G. M. *J. Org. Chem.* **1998**, *63*, 3821−3830.
(74) Hermans, J.; Wang, L. *J. Am. Chem. Soc.* **1997**, *119*, 10690−10697.
(75) Yu, Z. X.; Houk, K. N. *J. Am. Chem. Soc.* **2003**, *125*, 13825−13830.
(76) Harvey, J. N. *Faraday Discuss.* **2010**, *145*, 487−505.
(77) Ribeiro, A. J. M.; Ramos, M. J.; Fernandes, P. A. *J. Chem. Theory Comput.* **2010**, *6*, 2281−2292.
(78) Suárez, E.; Díaz, N.; Suárez, D. *J. Chem. Theory Comput.* **2011**, *7*, 2638−2653.
(79) Ribeiro, R. F.; Marenich, A. V.; Cramer, C. J.; Truhlar, D. G. *J. Phys. Chem. B* **2011**, *115*, 14556−14562.
(80) Hatanaka, M.; Morokuma, K. *J. Am. Chem. Soc.* **2013**, *135*, 13972−13979.
(81) Nakai, H.; Ishikawa, A. *J. Chem. Phys.* **2014**, *141*, 174106.
(82) Fukui, K. *J. Phys. Chem.* **1970**, *74*, 4161−4163.
(83) Ishida, K.; Morokuma, K.; Komornicki, A. *J. Chem. Phys.* **1977**, *66*, 2153−2156.
(84) Ohno, K.; Maeda, S. *Phys. Scr.* **2008**, *78*, 058122.
(85) Ohno, K.; Maeda, S. *Chem. Phys. Lett.* **2004**, *384*, 277−282.
(86) Maeda, S.; Osada, Y.; Morokuma, K.; Ohno, K. GRRM, a developmental version at Kyoto University.
(87) Frisch, M. J.; Trucks, G. W.; Schlegel, H. B.; Scuseria, G. E.; Robb, M. A.; Cheeseman, J. R.; Scalmani, G.; Barone, V.; Mennucci, B.; Petersson, G. A.; Nakatsuji, H.; Caricato, M.; Li, X.; Hratchian, Izmaylov, A. F.; Bloino, J.; Zheng, G.; Sonnenberg, J. L.; Hada, M.; Ehara, M.; Toyota, K.; Fukuda, R.; Hasegawa, J.; Ishida, M.; Nakajima, T.; Honda, Y.; Kitao, O.; Nakai, H.; Vreven, T.; Montgomery, J. A., Jr.; Peralta, J. E.; Ogliaro, F.; Bearpark, M.; Heyd, J. J.; Brothers, E.; Kudin, K. N.; Staroverov, V. N.; Keith, T.; Kobayashi, R.; Normand, J.; Raghavachari, K.; Rendell, A.; Burant, J. C.; Iyengar, S. S.; Tomasi, J.; Cossi, M.; Rega, N.; Millam, J. M.; Klene, M.; Knox, J. E.; Cross, J. B.; Bakken, V.; Adamo, C.; Jaramillo, J.; Gomperts, R.; Stratmann, R. E.; Yazyev, O.; Austin, A. J.; Cammi, R.; Pomelli, C.; Ochterski, J. W.; Martin, R. L.; Morokuma, K.; Zakrzewski, V. G.; Voth, G. A.; Salvador, P.; Dannenberg, J. J.; Dapprich, S.; Daniels, A. D.; Farkas, O.; Foresman, J. B.; Ortiz, J. V.; Cioslowski, J.; Fox, D. J. *Gaussian 09*, revision D.01; Gaussian Inc.: Wallingford, CT, 2009.
(88) Holden, M. S.; Crouch, R. D. *J. Chem. Educ.* **2001**, *78*, 1104−1105.
(89) Damkaci, F.; Szymaniak, A. *J. Chem. Educ.* **2014**, *91*, 943−945.
(90) Li, N.; Chen, X. H.; Song, J.; Luo, S. W.; Fan, W.; Gong, L. Z. *J. Am. Chem. Soc.* **2009**, *131*, 15301−15310.

DOI: 10.1021/acs.joc.5b00407
J. Org. Chem. 2015, 80, 6959−6967